Supporting Information

Non-crystalline Zeolitic Imidazolate Frameworks Tethered with Ionic Liquids as Catalysts for CO_2 Conversion into Cyclic Carbonates

Jinquan Wang[a], Xiukai Li[a], Guangshun Yi[a], Siew Ping Teong[a], Shook Pui Chan[a], Xinglong Zhang[b]*, Yugen Zhang[a]**

[a]*Institute of Sustainability for Chemicals, Energy and Environment (ISCE[2]), Agency for Science, Technology and Research (A*STAR), 1 Pesek Road Jurong Island, Singapore 627833.*

[b]*Institute of High Performance Computing (IHPC), Agency for Science, Technology and Research (A*STAR), 1 Fusionopolis Way, #16-16 Connexis, Singapore 138632, Singapore.*

[*]*E-mail: wang_jinquan@isce2.a-star.edu.sg(J.Wang), zhang_xinglong@ihpc.a-star.edu.sg (X. Zhang), zhang_yugen@isce2.a-star.edu.sg (Y. Zhang)*

II. COMPUTATIONAL SECTION

II.1 Computational Methods

The model system in the presence of one epoxide molecule was conformationally sampled to locate the most stable complex. The conformational sampling was carried out using Grimme's *CREST* program,[1,2] which used metadynamics (MTD) with genetic z-matrix crossing (GC) performed at the GFN2-xTB[3–5] extended semiempirical tight-binding level of theory with *opt= vtight* option.

The resulting GFN2-xTB optimized structures (12 in total) were further optimized, using *Gaussian 16* rev. B.01 software,[6] in the gas phase using the B3LYP hybrid functional[7–10] with Grimme's D3 dispersion correction with Becke-Johnson damping[11] (hereafter denoted B3LYP-D3BJ) and the def2-SVPD[12,13] Karlsruhe-family basis set for Br atom and def2-SVP[12,14] basis set for all other atoms (this mixed basis set is denoted BS1). The "D" in def2-SVPD basis set denotes diffuse functions which are important for the correct description of anionic electron distributions.[15–17] Dispersion correction (D3BJ) has been added to correctly capture non-covalent interactions.[18–21] Minima and transition structures on the potential energy surface (PES) were confirmed as such by harmonic frequency analysis, showing respectively zero and one imaginary frequency.

Gibbs energies were evaluated at the reaction temperature of 90 ºC, using Grimme's scheme of quasi-RRHO treatment of vibrational entropies[22], using the GoodVibes code[23]. Vibrational entropies of frequencies below 100 cm^{-1} were obtained according to a free rotor description, using a smooth damping function to interpolate between the two limiting descriptions.[22]

The free energies reported in *Gaussian* from gas-phase optimization were further corrected using standard concentration of 1 mol/L,[24] which were used in solvation calculations, instead of the gas-phase 1atm used by default in the *Gaussian* program.

To improve on the accuracy of the corrected Gibbs energy profile, single point (SP) calculations on the gas phase B3LYP-D3BJ/BS1 optimized geometries were performed at B3LYP-D3BJ with def2-TZVPD[12,13] basis set for Br atom and def2-TZVP[12,14] basis set for all other atoms (denoted BS2) in the implicit SMD continuum solvation model[25] for ethanol solvent that was used experimentally, to account for the effect of solvent on the potential energy surface. The final corrected Gibbs energy SMD(ethanol)-B3LYP-D3BJ/BS2//B3LYP-D3BJ/BS1 is used for discussion throughout. All Gibbs energy values in the text and figures are quoted in kcal mol^{-1}.

Non-covalent interactions (NCIs) were analyzed using NCIPLOT[26] calculations. The *.wfn* files for NCIPLOT were generated at BS1 level of theory. NCI indices calculated with NCIPLOT were visualized at a gradient isosurface value of $s = 0.5$ au. These are colored according to the sign of the second eigenvalue (λ_2) of the Laplacian of the density ($\nabla^2\rho$) over the range of –0.1 (blue = attractive) to +0.1 (red = repulsive). Molecular orbitals are visualized using an isosurface value of 0.05 au throughout. All molecular structures and molecular orbitals were visualized using *PyMOL* software.[27]

Geometries of all optimized structures (in *.xyz* format with their associated energy in Hartrees) are included in a separate folder named *DFT_optimized_structures* with an associated

readme.txt file. All these data have been deposited with this Supporting Information and uploaded to https://zenodo.org/records/10399395 (DOI: 10.5281/zenodo.10399395).

II.2 Model reaction

Scheme S1 shows the model reaction that we have used for the computational studies of reaction mechanism for ZIF catalyzed conversion of CO_2 and epoxide to cyclic carbonate. Model catalyst **M3** was used to represent the full catalyst **Z3**.

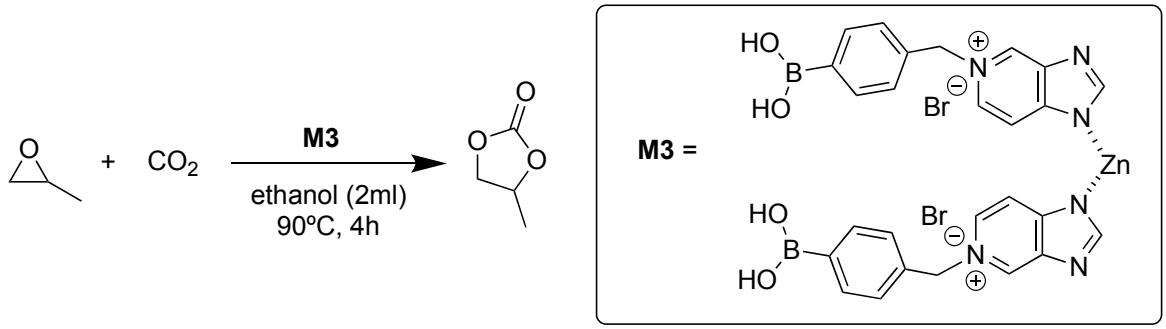

Scheme S1. Model reaction used in the computational modelling studies.

The DFT optimized structures for the model reaction is shown in Figure S7. The ring opening of Zn-coordinated epoxide by the bromide anion (**TS1**) has a much lower barrier than the ring opening of boronic acid coordinated epoxide (**TS1ba** and **TS1baL**). In **TS1ba**, the Zn is tri-coordinated whereas in **TS1baL**, the tetrahedral coordination of Zn ion is fulfilled by coordinating an ethanol solvent molecule. **TS1baL** has a slightly lower barrier than **TS1ba**, however, both barriers are much higher than **TS1**.

TS1	**TS1ba**
$\Delta G^{\ddagger}$ = 15.2	$\Delta G^{\ddagger}$ = 27.8
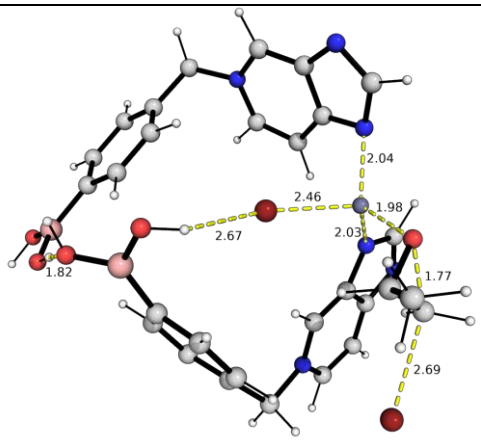	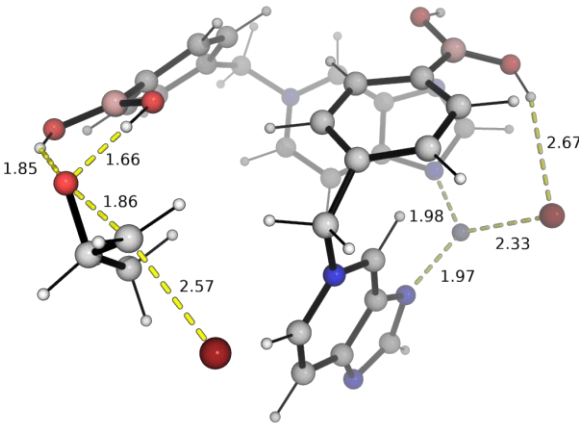
TS1baL	**TS2**
$\Delta G^{\ddagger}$ = 26.7	$\Delta G^{\ddagger}$ = 7.8

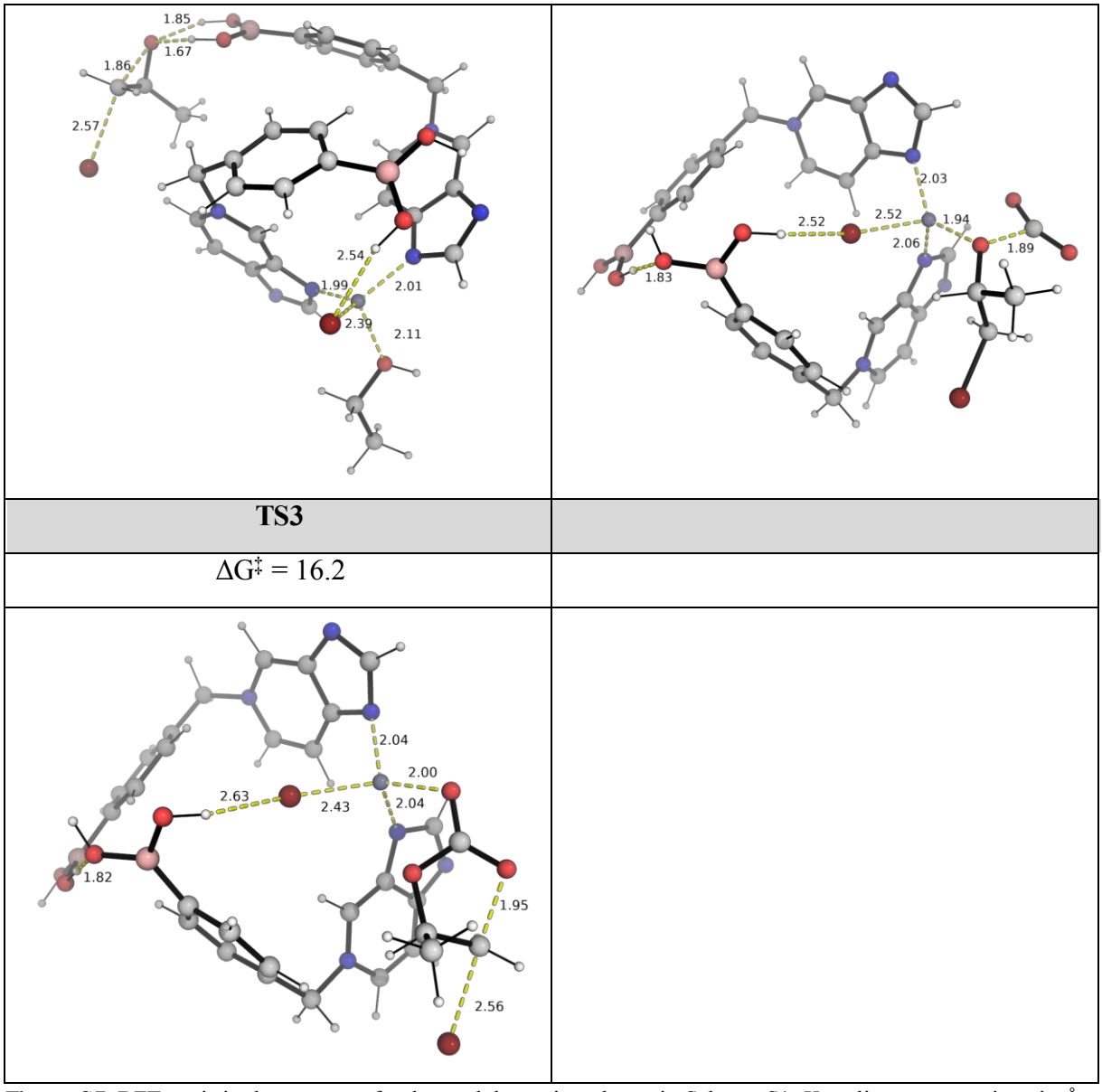

Figure S7. DFT optimized structures for the model reaction shown in Scheme S1. Key distances are given in Å.

II.3 Role of boronic acid groups

To understand the role of boronic acid groups on the catalyst, we replaced the boronic acid group by the methyl group and the reaction is shown in Scheme S2.

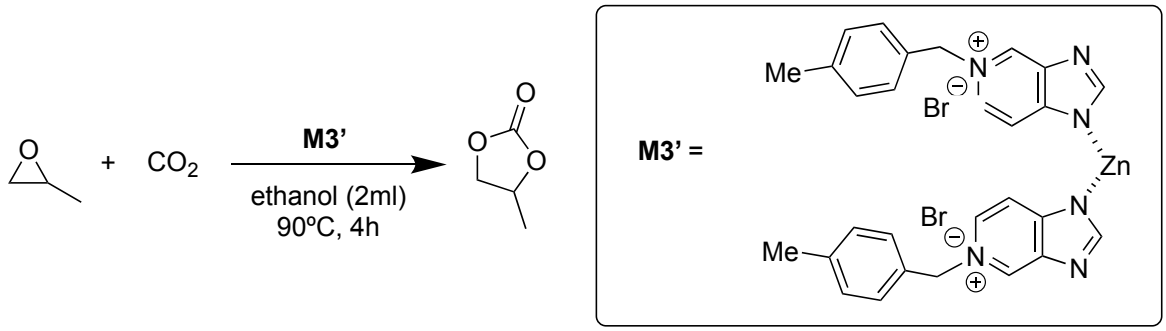

Scheme S2. Reaction where the boronic acid groups in the catalyst is replaced by methyl groups.

The full Gibbs energy profile for this model reaction is shown in Figure S8. Similar to the model reaction in Scheme S1, with the corresponding Gibbs energy profile in main text Figure 4, the ring closure step is the rate-determining step. This reaction gives an energetic span of 23.4 kcal/mol, which is 5.0 kcal/mol higher than the energetic span of the model reaction (18.4 kcal/mol, Figure 4, main text). This indicates that the boronic acid groups help with lowering the energetic span of the overall catalytic reaction.

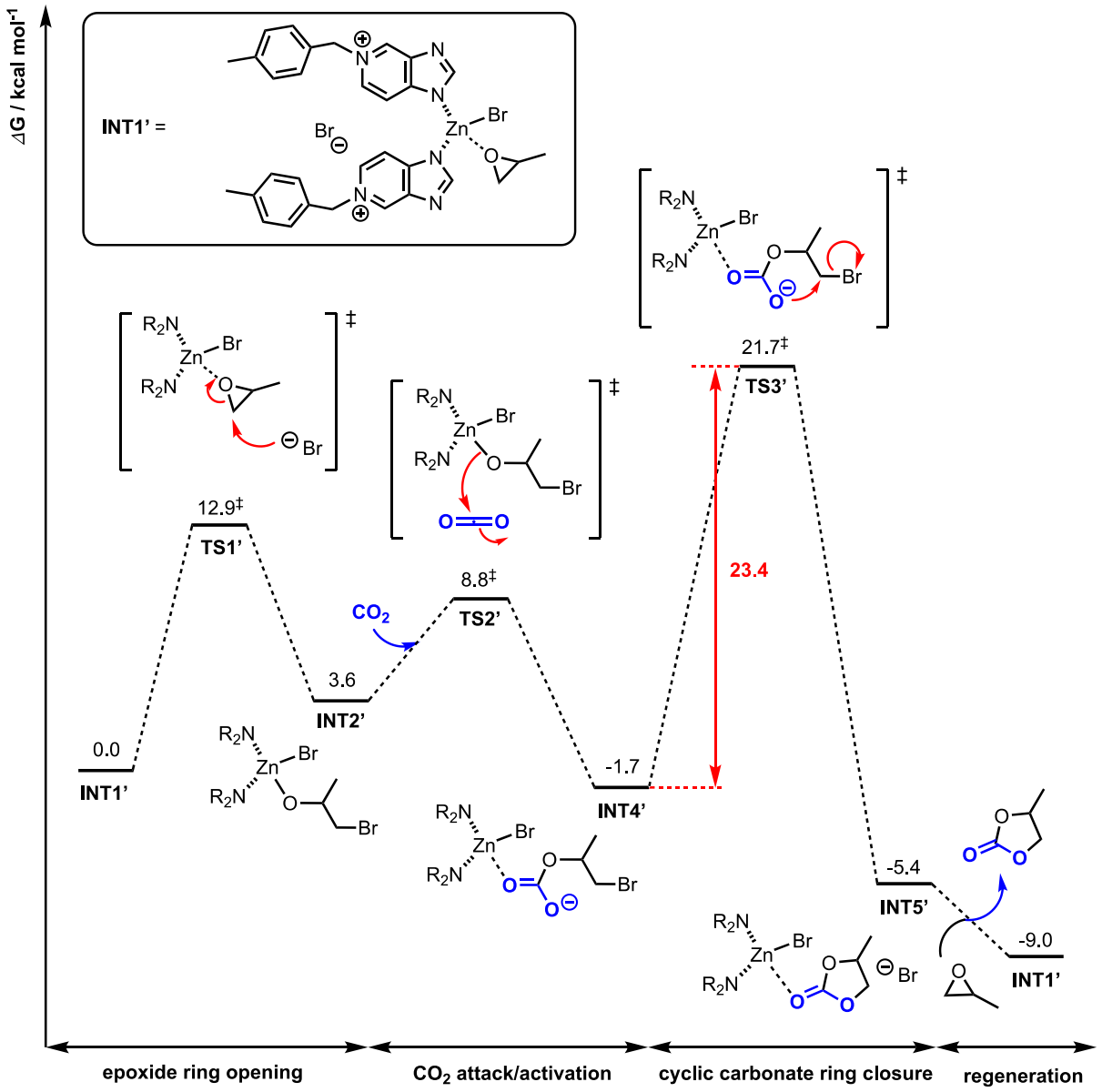

Figure S8. Gibbs energy profile for the reaction shown in Scheme S2.

II.4 Model reaction based on catalyst Z1

We focused on the turnover frequency (TOF)-determining intermediate (TDI), which is the Zn-coordinated complex after CO_2 addition (**INT4z**, Scheme S3), and the TOF-determining

transition state (TDTS), which is the ring closure step for the model reaction using catalyst **Z1** (**TS3z**, Scheme S3).

This gives the energetic span of 19.4 kcal/mol, which is 1.0 kcal/mol higher than the energetic span calculated for the model reaction for catalyst **Z3**.

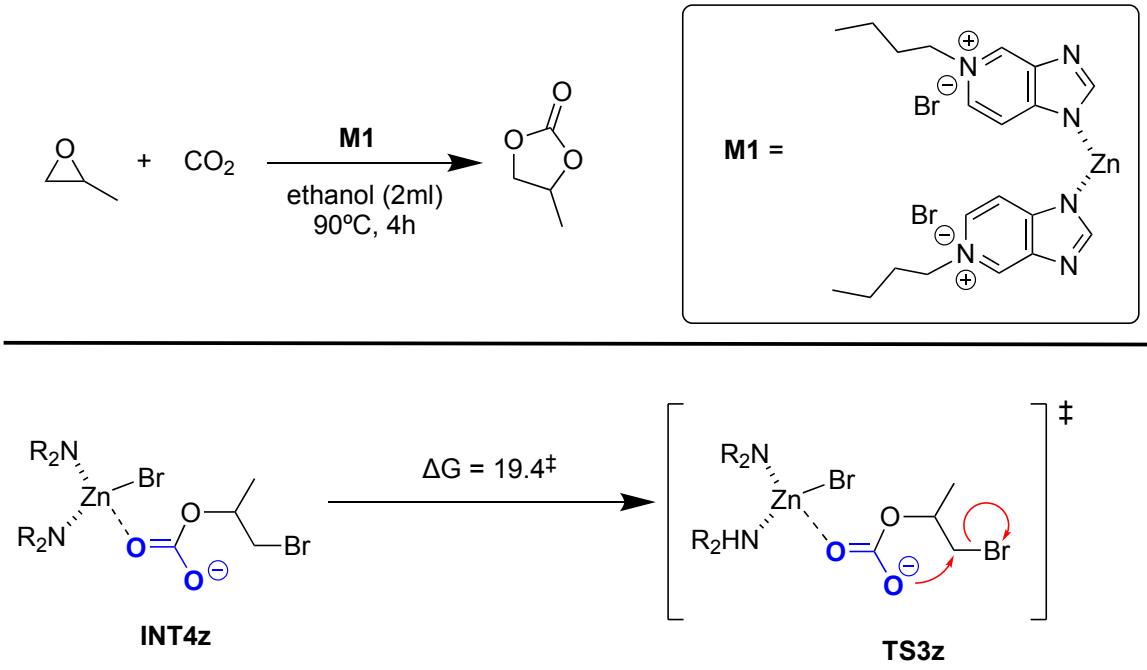

Scheme S3. Model reaction based on catalyst **Z1** and the key step for determining the energetic span.

II.5 Molecular origins of contributions by boronic acid groups

To further understand the molecular origins of the roles of the boronic acid groups, we performed the highest occupied molecular orbitals (HOMO) and non-covalent interactions (NCI) analysis for the key TSs resulting from reactions in Schemes S1–3 (**TS3**, **TS3'** and **TS3z**). The results are shown in Figure S9.

TS3	TS3'	TS3z
DFT optimized structures		
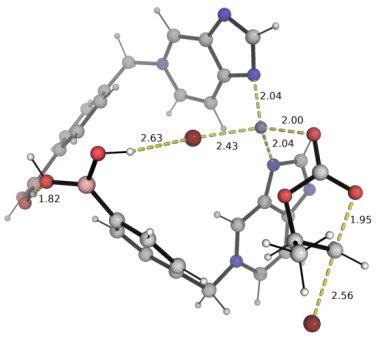	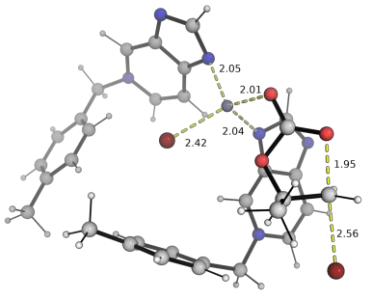	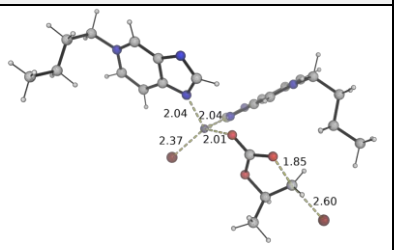
HOMOs		

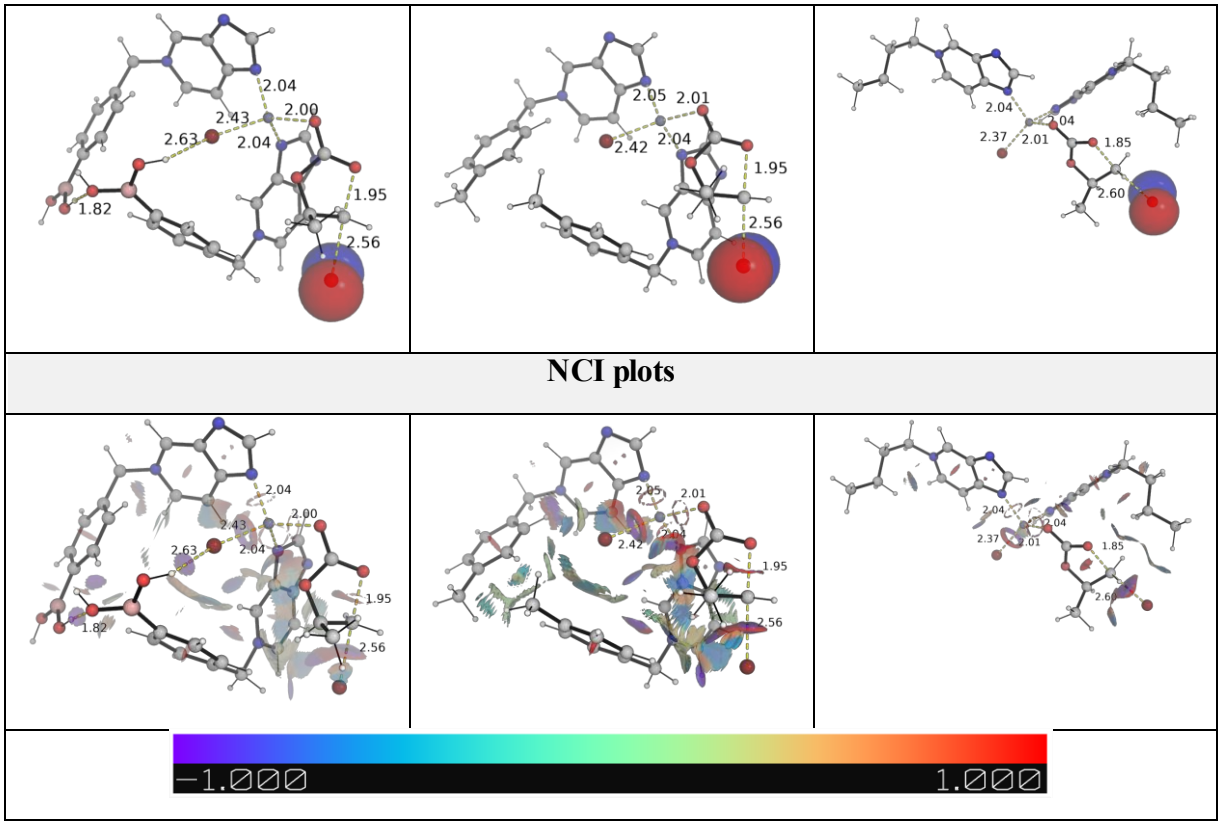

Figure S9. DFT optimized structures, HOMOs and NCI plots for the key TSs resulting from reactions in Schemes S1–3. Key distances are given in Å.

II.6 Optimized structures and absolute energies, zero-point energies

Geometries of all optimized structures (in *.xyz* format with their associated energy in Hartrees) are included in a separate folder named *DFT_optimized_structures* with an associated readme.txt file. All these data have been deposited and uploaded to https://zenodo.org/records/10399395 (DOI: 10.5281/zenodo.10399395).

Absolute values (in Hartrees) for SCF energy, zero-point vibrational energy (ZPE), enthalpy and quasi-harmonic Gibbs free energy (at 90 °C/363.15 K) for optimized structures are given below. Single point corrections in SMD ethanol using B3LYP-D3/BS2 level of theory are also included.

Structure	E/au	ZPE/au	H/au	T.S/au	qh-G/au	SP B3LYP-D3/BS2
CO2	-188.44468	0.011776	-188.42837	0.026724	-188.455093	-188.6672
epoxide	-192.97454	0.085035	-192.88226	0.036821	-192.919077	-193.2052
cyclic_carbonate	-381.4548	0.102874	-381.3421	0.044682	-381.386477	-381.9099
dimer_sm_epoxide	-8803.658	0.576725	-8803.0186	0.170469	-8803.172421	-8806.657345

dimer_sm_epoxide_c2	-8803.658	0.576725	-8803.0186	0.170458	-8803.172417	-8806.657342
dimer_sm_epoxide_c3	-8803.6588	0.576931	-8803.0194	0.168919	-8803.172449	-8806.657071
dimer_sm_epoxide_c4	-8803.6588	0.576931	-8803.0194	0.168917	-8803.172448	-8806.65708
dimer_sm_epoxide_c5	-8803.6588	0.576932	-8803.0194	0.168915	-8803.172446	-8806.657075
dimer_sm_epoxide_c6	-8803.6588	0.576932	-8803.0194	0.168912	-8803.172445	-8806.657077
dimer_sm_epoxide_c7	-8803.6565	0.576853	-8803.0173	0.169754	-8803.170675	-8806.659842
dimer_sm_epoxide_c8	-8803.6525	0.576448	-8803.0132	0.171203	-8803.167401	-8806.653085
dimer_sm_epoxide_c9	-8803.6494	0.575706	-8803.0107	0.173077	-8803.165891	-8806.657583
dimer_sm_epoxide_c10	-8803.6494	0.575711	-8803.0107	0.173053	-8803.165877	-8806.657596
dimer_sm_epoxide_c11	-8803.6478	0.575914	-8803.0089	0.173903	-8803.164386	-8806.65798
dimer_sm_epoxide_c12	-8803.6434	0.575445	-8803.0048	0.17327	-8803.160201	-8806.655768
INT1	-8803.6622	0.5767	-8803.0231	0.169633	-8803.176726	-8806.6519
TS1	-8803.6341	0.575809	-8802.9966	0.167338	-8803.14824	-8806.6363
INT2	-8803.6616	0.576871	-8803.023	0.167632	-8803.174706	-8806.6641
INT3	-8992.1243	0.589972	-8991.4673	0.181392	-8991.630027	-8995.340613
TS2	-8992.1212	0.590345	-8991.4653	0.176885	-8991.624904	-8995.336051
INT4	-8992.1328	0.592595	-8991.4747	0.176807	-8991.634108	-8995.354331
TS3	-8992.1077	0.592314	-8991.4508	0.173704	-8991.608047	-8995.326162
INT5	-8992.134	0.594371	-8991.4744	0.178396	-8991.63412	-8995.355012
INT1ba	-8803.6349	0.576292	-8802.996	0.170084	-8803.149648	-8806.6402
TS1ba	-8803.5987	0.575491	-8802.9619	0.166795	-8803.113175	-8806.615906
INT2ba	-8803.6126	0.575122	-8802.9765	0.165189	-8803.126618	-8806.6338
TS1baL	-8958.5739	0.65744	-8957.8474	0.185301	-8958.014143	-8961.7657

z1_dimer_sm_epoxide	-8225.7528	0.533199	-8225.1679	0.149641	-8225.302092	-8228.092418
z1_dimer_sm_epoxide_c2	-8225.7528	0.533199	-8225.1679	0.149626	-8225.302085	-8228.092418
z1_dimer_sm_epoxide_c3	-8225.7528	0.5332	-8225.1679	0.149595	-8225.302072	-8228.092414
z1_dimer_sm_epoxide_c4	-8225.7529	0.53324	-8225.1679	0.149665	-8225.3022	-8228.091866
z1_dimer_sm_epoxide_c5	-8225.7529	0.533241	-8225.1679	0.14964	-8225.302186	-8228.091869
z1_dimer_sm_epoxide_c6	-8225.7541	0.533611	-8225.169	0.147112	-8225.301938	-8228.092031
z1_dimer_sm_epoxide_c7	-8225.7541	0.533613	-8225.169	0.147105	-8225.301932	-8228.09203
z1_dimer_sm_epoxide_c8	-8225.7541	0.533613	-8225.169	0.147105	-8225.301933	-8228.092029
z1_dimer_sm_epoxide_c9	-8225.7541	0.533614	-8225.169	0.147098	-8225.301928	-8228.092025
z1_dimer_sm_epoxide_c10	-8225.7539	0.533692	-8225.1687	0.147045	-8225.301528	-8228.09215
z1_dimer_sm_epoxide_c11	-8225.7543	0.533769	-8225.1691	0.146395	-8225.301668	-8228.091431
z1_dimer_sm_epoxide_c12	-8225.7543	0.53377	-8225.1691	0.146377	-8225.30166	-8228.091426
TS3z	-8414.1955	0.548676	-8413.5924	0.159021	-8413.733581	-8416.7701
INT4z	-8414.2402	0.549631	-8413.6362	0.154154	-8413.775104	-8416.8042
INT1'	-8530.4349	0.580568	-8529.7959	0.1635	-8529.942166	-8533.0963

TS1'	-8530.3995	0.578795	-8529.7625	0.168359	-8529.910639	-8533.071908
INT2'	-8530.4209	0.580148	-8529.7829	0.162717	-8529.928117	-8533.091036
TS2'	-8718.8835	0.593306	-8718.2282	0.17671	-8718.383768	-8721.766873
INT4'	-8718.8961	0.595715	-8718.2385	0.177131	-8718.39404	-8721.785948
TS3'	-8718.8683	0.595757	-8718.2119	0.167518	-8718.362147	-8721.752738
INT5'	-8718.9036	0.597667	-8718.2445	0.177341	-8718.39954	-8721.793926

II.7 References for computational section:

Full reference Gaussian 16:

Gaussian 16, Revision B.01, Frisch, M. J.; Trucks, G. W.; Schlegel, H. B.; Scuseria, G. E.; Robb, M. A.; Cheeseman, J. R.; Scalmani, G.; Barone, V.; Mennucci, B.; Petersson, G. A.; Nakatsuji, H.; Caricato, M.; Li, X.; Hratchian, H. P.; Izmaylov, A. F.; Bloino, J.; Zheng, G.; Sonnenberg, J. L.; Hada, M.; Ehara, M.; Toyota, K.; Fukuda, R.; Hasegawa, J.; Ishida, M.; Nakajima, T.; Honda, Y.; Kitao, O.; Nakai, H.; Vreven, T.; Montgomery Jr., J. A.; Peralta, J. E.; Ogliaro, F.; Bearpark, M.; Heyd, J. J.; Brothers, E.; Kudin, K. N.; Staroverov, V. N.; Kobayashi, R.; Normand, J.; Raghavachari, K.; Rendell, A.; Burant, J. C.; Iyengar, S. S.; Tomasi, J.; Cossi, M.; Rega, N.; Millam, J. M.; Klene, M.; Knox, J. E.; Cross, J. B.; Bakken, V.; Adamo, C.; Jaramillo, J.; Gomperts, R.; Stratmann, R. E.; Yazyev, O.; Austin, A. J.; Cammi, R.; Pomelli, C.; Ochterski, J. W.; Martin, R. L.; Morokuma, K.; Zakrzewski, V. G.; Voth, G. A.; Salvador, P.; Dannenberg, J. J.; Dapprich, S.; Daniels, A. D.; Farkas, Ö.; Foresman, J. B.; Ortiz, J. V; Cioslowski, J.; Fox, D. J. Gaussian, Inc., Wallingford CT, 2016.

(1) Grimme, S. Exploration of Chemical Compound, Conformer, and Reaction Space with Meta-Dynamics Simulations Based on Tight-Binding Quantum Chemical Calculations. *J. Chem. Theory Comput.* **2019**, *15* (5), 2847–2862.

(2) Pracht, P.; Bohle, F.; Grimme, S. Automated Exploration of the Low-Energy Chemical Space with Fast Quantum Chemical Methods. *Phys. Chem. Chem. Phys.* **2020**, *22* (14), 7169–7192.

(3) Bannwarth, C.; Ehlert, S.; Grimme, S. GFN2-XTB - An Accurate and Broadly Parametrized Self-Consistent Tight-Binding Quantum Chemical Method with Multipole Electrostatics and Density-Dependent Dispersion Contributions. *J. Chem. Theory Comput.* **2019**, *15* (3), 1652–1671.

(4) Grimme, S.; Bannwarth, C.; Shushkov, P. A Robust and Accurate Tight-Binding Quantum Chemical Method for Structures, Vibrational Frequencies, and Noncovalent Interactions of Large Molecular Systems Parametrized for All Spd-Block Elements (Z = 1-86). *J. Chem. Theory Comput.* **2017**, *13* (5), 1989–2009.

(5) Bannwarth, C.; Caldeweyher, E.; Ehlert, S.; Hansen, A.; Pracht, P.; Seibert, J.; Spicher, S.; Grimme, S. Extended Tight-Binding Quantum Chemistry Methods. *Wiley Interdiscip. Rev. Comput. Mol. Sci.* **2021**, *11* (2), e1493.

(6) Frisch, M. J. .; Trucks, G. W. .; Schlegel, H. B. .; Scuseria, G. E. .; Robb, M. A. .; Cheeseman, J. R. .; Scalmani, G. .; Barone, V. .; Petersson, G. A. .; Nakatsuji, H. .; et al. Gaussian 16, Revision B.01. 2016.

(7) Becke, A. D. Density-Functional Thermochemistry. III. The Role of Exact Exchange. *J. Chem. Phys.* **1993**, *98* (7), 5648–5652.

(8) Lee, C.; Yang, W.; Parr, R. G. Development of the Colle-Salvetti Correlation-Energy Formula into a Functional of the Electron Density. *Phys. Rev. B* **1988**, *37* (2), 785–789.

(9) Vosko, S. H.; Wilk, L.; Nusair, M. Accurate Spin-Dependent Electron Liquid Correlation Energies for Local Spin Density Calculations: A Critical Analysis. *Can. J. Phys.* **1980**, *58* (8), 1200–1211.

(10) Stephens, P. J.; Devlin, F. J.; Chabalowski, C. F.; Frisch, M. J. Ab Initio Calculation of Vibrational Absorption and Circular Dichroism Spectra Using Density Functional Force Fields. *J. Phys. Chem.* **1994**, *98* (45), 11623–11627.

(11) Grimme, S.; Antony, J.; Ehrlich, S.; Krieg, H. A Consistent and Accurate Ab Initio Parametrization of Density Functional Dispersion Correction (DFT-D) for the 94 Elements H-Pu. *J. Chem. Phys.* **2010**, *132* (15), 154104.

(12) Weigend, F.; Ahlrichs, R. Balanced Basis Sets of Split Valence, Triple Zeta Valence and Quadruple Zeta Valence Quality for H to Rn: Design and Assessment of Accuracy. *Phys. Chem. Chem. Phys.* **2005**, *7* (18), 3297–3305.

(13) Hellweg, A.; Rappoport, D. Development of New Auxiliary Basis Functions of the Karlsruhe Segmented Contracted Basis Sets Including Diffuse Basis Functions (Def2-SVPD, Def2-TZVPPD, and Def2-QVPPD) for RI-MP2 and RI-CC Calculations. *Phys. Chem. Chem. Phys.* **2014**, *17* (2), 1010–1017.

(14) Weigend, F. Accurate Coulomb-Fitting Basis Sets for H to Rn. *Phys. Chem. Chem. Phys.* **2006**, *8* (9), 1057–1065.

(15) Davidson, E. R.; Feller, D. Basis Set Selection for Molecular Calculations. *Chem. Rev.* **1986**, *86* (4), 681–696.

(16) Lynch, B. J.; Zhao, Y.; Truhlar, D. G. Effectiveness of Diffuse Basis Functions for Calculating Relative Energies by Density Functional Theory. *J. Phys. Chem. A* **2003**, *107* (9), 1384–1388.

(17) Papajak, E.; Zheng, J.; Xu, X.; Leverentz, H. R.; Truhlar, D. G. Perspectives on Basis Sets Beautiful: Seasonal Plantings of Diffuse Basis Functions. *J. Chem. Theory Comput.* **2011**, *7* (10), 3027–3034.

(18) Grimme, S. Density Functional Theory with London Dispersion Corrections. *Wiley Interdiscip. Rev. Comput. Mol. Sci.* **2011**, *1* (2), 211–228.

(19) Burns, L. A.; Vázquez-Mayagoitia, Á.; Sumpter, B. G.; Sherrill, C. D. Density-Functional Approaches to Noncovalent Interactions: A Comparison of Dispersion Corrections (DFT-D), Exchange-Hole Dipole Moment (XDM) Theory, and Specialized Functionals. *J. Chem. Phys.* **2011**, *134* (8).

(20) Dilabio, G. A.; Koleini, M. Dispersion-Correcting Potentials Can Significantly Improve the Bond Dissociation Enthalpies and Noncovalent Binding Energies Predicted by Density-Functional Theory. *J. Chem. Phys.* **2014**, *140* (18).

(21) Cohen, A. J.; Mori-Sánchez, P.; Yang, W. Challenges for Density Functional Theory.

Chem. Rev. **2012**, *112* (1), 289–320.

(22) Grimme, S. Supramolecular Binding Thermodynamics by Dispersion-Corrected Density Functional Theory. *Chem.: Eur. J.* **2012**, *18* (32), 9955–9964.

(23) Luchini, G.; Alegre-Requena, J. V.; Funes-Ardoiz, I.; Paton, R. S.; Pollice, R. GoodVibes: Automated Thermochemistry for Heterogeneous Computational Chemistry Data. **2020**, *9*, 291.

(24) Bryantsev, V. S.; Diallo, M. S.; Goddard Iii, W. A.; Goddard, W. A. Calculation of Solvation Free Energies of Charged Solutes Using Mixed Cluster/Continuum Models. *J. Phys. Chem. B* **2008**, *112* (32), 9709–9719.

(25) Marenich, A. V.; Cramer, C. J.; Truhlar, D. G. Universal Solvation Model Based on Solute Electron Density and on a Continuum Model of the Solvent Defined by the Bulk Dielectric Constant and Atomic Surface Tensions. *J. Phys. Chem. B* **2009**, *113* (18), 6378–6396.

(26) Contreras-García, J.; Johnson, E. R.; Keinan, S.; Chaudret, R.; Piquemal, J. P.; Beratan, D. N.; Yang, W. NCIPLOT: A Program for Plotting Noncovalent Interaction Regions. *J. Chem. Theory Comput.* **2011**, *7* (3), 625–632.

(27) Schrödinger, L. *The PyMOL Molecular Graphics Development Component, Version 1.8*; 2015.